

## ANALYSIS OF PERIODIC OPTICAL VARIABILITY IN THE COMPACT X-RAY SOURCE HER X-1/HZ HERCULIS

J. DEETER, L. CROSA, D. GEREND, AND P. E. BOYNTON

Department of Astronomy, University of Washington, Seattle

Received 1975 August 25

### ABSTRACT

Analysis of the large pool of optical photometric data now available on the X-ray binary Her X-1/HZ Her reveals considerable variability on a time scale of hours. These flux variations are found to repeat in a highly regular fashion over the 35<sup>d</sup> X-ray ON-OFF cycle. The frequency composition and symmetry properties of this pattern suggest that the time dependence results from the uniformly changing orientation of luminous elements in this system.

*Subject headings:* binaries — stars: individual — X-rays: sources

### I. INTRODUCTION

Previously we discussed properties of the optical light curve of HZ Herculis deduced from color photometric observations of this galactic X-ray source (Boynton *et al.* 1973). Many of the ideas investigated in that paper were motivated by the prescient work of Kurochkin (1972, 1973). Our principal conclusions concerned the strong morphological and color changes that are clearly correlated with the  $\sim 35^d$  X-ray flux cycle. Subsequently, several authors have corroborated the observation of a well-defined secondary minimum at midorbital phase ( $\phi = 0.5$ ) during the X-ray ON state, and a bright, sharply peaked feature during the OFF state as shown in Figures 1*b* and 1*c* (Chevalier and Ilovaisky 1973, 1974*a*; Grandi *et al.* 1974). The resulting modulation of optical flux at midphase is roughly 50 percent in the *U* band, and significantly less in *B*, *V*, and *r*. This color distinction, along with that associated with the light at primary minimum ( $\phi = 0.0$ ), suggested a system with three luminosity sources: the relatively cool back side of the primary star, its heated face which is responsible for a large fraction of the 1<sup>d</sup>7 flux variation, and finally superposed structure on the light curve which is strongest around midphase, but varies systematically over the 35<sup>d</sup> cycle. The secondary minimum was tentatively identified with the occultation of the heated face by an accretion disk associated with the compact companion.

In the present paper we suggest that various bumps, shoulders, peaks, the shape of primary minima, and general asymmetries in the light curve discussed previously in the literature are all part of a single pattern. These morphological variations (shown as departures from a lower envelope curve in Fig. 1*d*) result from a continuous, predictable progression toward earlier phase of large-amplitude bright features. This periodic structure along with the regular occurrence of a secondary minimum results in a strikingly repeatable evolution of the 1<sup>d</sup>7 light curve through the  $\sim 35^d$  cycle. The harmonic content and symmetry properties of this varying component strongly suggest

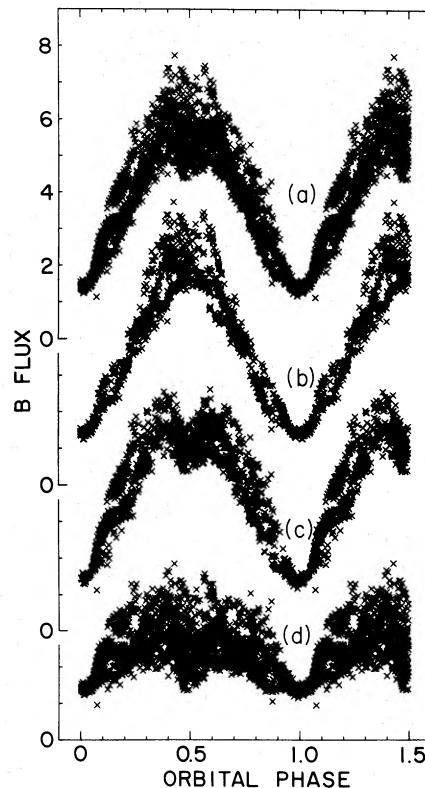


FIG. 1.—(a) All *B* data shown as optical flux (as defined in Boynton *et al.* 1973) modulo 1<sup>d</sup>7; 1.5 orbits are shown to better display behavior around primary minimum. (b) All *B* data within the 17.5 day interval roughly centered on the X-ray inactive period. (c) All *B* data within the 17.5 day interval roughly centered on the X-ray active period. (d) Same as Fig. 1*a* with lower envelope curve [approximated by  $1.5(1 - \cos 2\pi\phi)$ ] subtracted.

a geometrical interpretation for the optical behavior of this source.

## II. 35 DAY EVOLUTION OF THE OPTICAL LIGHT CURVE

### a) Observations

The data set which forms the observational basis of this work includes the photoelectric photometry of Davidsen *et al.* (1972), Petro and Hiltner (1973), Grandi *et al.* (1974), Lyutiy, Sunyaev, and Cherepashchuk (1973, 1974), and Chevalier and Ilovaisky (1974*b*), as well as 85 nights of our own data from the 78 cm reflector of the University of Washington. From this multicolor data set, the 2001 *B* flux measurements span the 1972, 1973, and 1974 observing seasons with a total of 250 nights distributed through 16 X-ray ON-OFF cycles. We find these *B* observations adequate to construct light curves for each of the nominal 20 orbits in the X-ray ON-OFF cycle. A striking time-reversal symmetry is visually evident in this sequence of curves. There are two "reflection points," occurring approximately three and 13 orbits after X-ray turn-on. This symmetry, which was apparent in the 1972 data and has recently been qualitatively noted by Chevalier and Ilovaisky (1974*a*), defines a natural epoch for the optical 35<sup>d</sup> phase. If  $\phi$  and  $\psi$  are used to denote 1<sup>d</sup>7 and 35<sup>d</sup> phase, respectively, then the epoch for  $\psi$  has been chosen so that these two reflection points correspond to  $\psi = 0.0$  and  $\psi = 0.5$ . This epoch has been used in labeling Figure 2, where we have also exploited the symmetry to superpose appropriate pairs of the 20 light curves. (It is evident in Fig. 2 that the orbits corresponding to the two symmetry points are themselves symmetric in orbital phase. Thus there are actually four symmetry points, corresponding to  $\phi = 0.0$  and  $\phi = 0.5$  in each of the two symmetric light curves.) Since we are primarily interested in variations from one orbit to the next, in Figure 2 we have subtracted the 1<sup>d</sup>7 fixed lower envelope curve in the same way that produces Figure 1*d*. The interval between observed or interpolated X-ray turn-ons has been divided into 20 equal bins, thereby yielding 20 light curves regardless of the number of orbits in a particular X-ray cycle.

From Figure 2 we see that the central peak and secondary minimum of Figure 1*b*, *c* are only mid-phase aspects of a more general pattern of features which pervade the light curve throughout the 35<sup>d</sup> cycle. While the partitioning of data between Figures 1*b* and 1*c* yields some clues to the nature of the large dispersion in flux at midorbital phase in Figure 1*a*, the finer partitioning in Figure 2 shows that the residual scatter in flux for *all* values of orbital phase (see Fig. 1*d*) is largely systematic, not stochastic. This conclusion is supported by the obvious agreement between data from many different 35<sup>d</sup> cycles which are superposed to form each member of the set of 20 curves (see Fig. 3). Also there are a number of instances in which data do not overlap in orbital phase but form adjacent portions of these curves whose continuity is then striking evidence for the regularity and per-

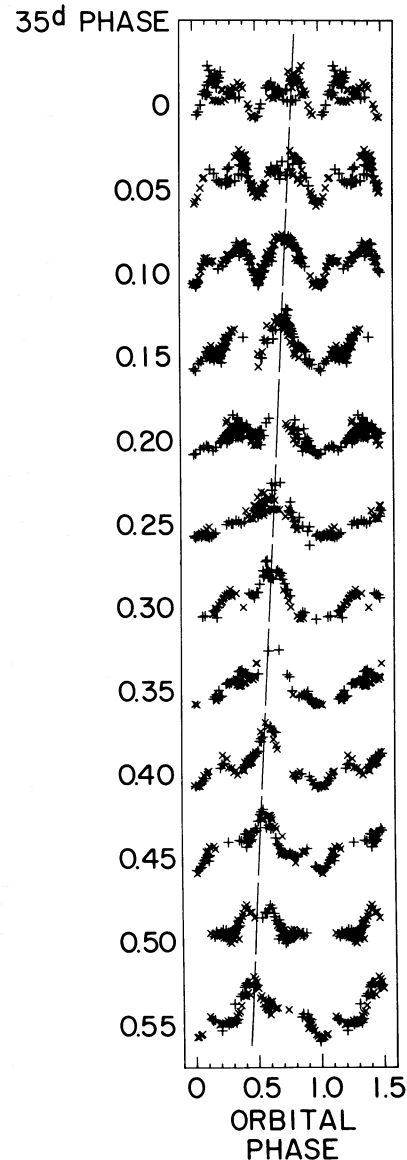


FIG. 2.—All *B* flux data reduced to 946 points by averaging over 40 minute intervals in time. Each curve is plotted modulo the 1<sup>d</sup>7 orbital period and represents 0.05 phase intervals of the  $\sim 35^d$  X-ray cycle. The first curve is centered at the symmetry epoch,  $\psi = 0$ , i.e.,  $\sim 3$  orbits after X-ray turn-on. Each curve is the superposition of two curves according to the time-reversal symmetry  $F_B(-\phi, -\psi) = F_B(\phi, \psi)$ . That is, the 20th (last) curve is reflected and superposed on the second, the 19th on the third, etc.; and the first and eleventh are self-reflected. Thus only eleven curves are necessary to represent all the data, but twelve are given to show the behavior through the symmetry point at  $\psi = 0.5$ . Direct (unreflected) points are indicated by  $\times$ ; reflected points by  $+$ .

sistence of the shape of these curves. It seems important to emphasize that the structure in Figure 2 is not a minor perturbation on the basic 1<sup>d</sup>7 light curve. On the contrary, the maximum amplitude of these features is roughly half the amplitude of the basic 1<sup>d</sup>7 variation (compare Fig. 1*a* and Fig. 1*d*).

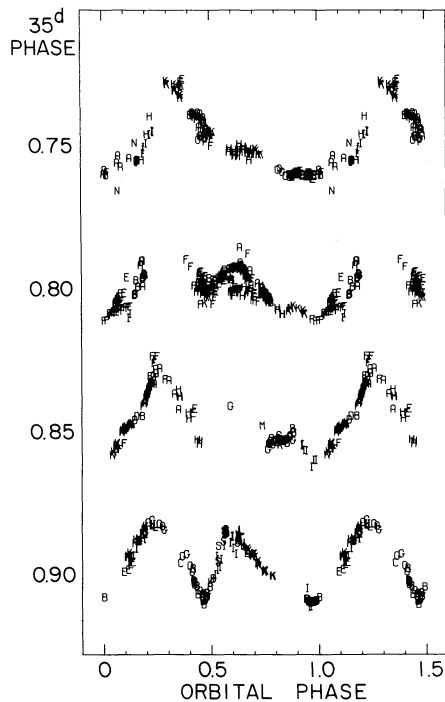


FIG. 3.—Expanded view of a portion of Fig. 2, showing only direct (unreflected) points. Each letter corresponds to a distinct  $35^{\text{d}}$  X-ray ON-OFF cycle. From top to bottom, these four curves contain points from 9, 7, 9, and 8 different  $35^{\text{d}}$  periods.

An interesting pattern is suggested by visual inspection of the successive light curves in Figure 2. There are some features which appear to drift continuously toward earlier orbital phase. The progression of the strongest peak (indicated by the diagonal line in Fig. 2) can be followed through the entire  $35^{\text{d}}$  cycle. If these features move regularly (coherently) from  $35^{\text{d}}$  cycle to  $35^{\text{d}}$  cycle this slope *must* be a ratio of integers, otherwise the pattern would be smeared in stacking many  $35^{\text{d}}$  periods (the superposition modulo  $35^{\text{d}}$  was based on observed and interpolated X-ray turn-on times). On the other hand, if physical conditions which produce this pattern are *restored* every 35 days and gradually relax in the interim, no such constraint is necessary. In fact the progression of features from curve to curve is so clearly present, and violation of that pattern so infrequent, that even in the absence of overlapping data from various  $35^{\text{d}}$  cycles, the reality of this effect seems well established.

In contrast to this motion of bright features, the secondary minimum appears relatively stationary in 197 phase, exhibiting only small displacements as bright features pass through. This behavior seems consistent with an occulting feature which is stationary in the corotating orbital frame.

#### b) Time Series Analysis

In an attempt to understand the time-dependent properties of the structure on the light curve suggested in Figure 2, we have examined the power spectrum

of the 1973 *B* data which span 255 days. Observations were binned in 40 minute intervals, leaving a large fraction of empty bins. The periodic content of this sampling is dominated by diurnal and to a lesser extent by lunar constraints on astronomical observing. The frequency domain representation of sampling structure, the window function, is shown in Figure 4a. This is simply the power spectrum of the data with amplitudes of 1 or 0 for bins with or without data, respectively, and as expected, shows considerable power at  $1 \text{ day}^{-1}$  and harmonics thereof. Because this sampling structure modulates the amplitude of the *B*-flux time series, the window function appears as side-band structure on every spectral feature in the data. Figure 4b shows this effect on the dominant  $\nu_{1.7} = (1/1.7) \text{ day}^{-1}$  line in the HZ Her light curve. By successively subtracting the largest of the remaining frequency components from the data, the associated side-band structure is also removed, reducing the clutter in the power spectrum and allowing smaller and smaller amplitude features to be identified. This cleaning method leads to the “uncovering” of the spectral lines shown in Figures 4c and 4d. We find the results of this spectral sifting somewhat surprising:

a) Virtually all power is concentrated at the discrete frequencies  $\nu_{1.7}$  and sums of harmonics of  $\nu_{1.7}$  and  $\nu_{35}$ . Each of the five lines shown in Figures 4b and 4c is significant at the 1 percent level or better when compared to the local distribution of power per bin. Furthermore, taken together they contain roughly 95 percent of the total power in the spectrum.

b) These strong lines represent a clear dominance of positive sidebands (frequency sums as distinguished from differences) in the spectrum. This tendency is consistent with the observation that features drift toward earlier phase.

c) Finally, there is a conspicuous absence of power at  $\nu_{35}$ , indicating that, in spite of the degree of  $35^{\text{d}}$  modulation at midphase, the average flux per orbit does not change through the 35 day X-ray cycle by more than a few percent of the amplitude of the 1.7 day variation.

Further application of this analysis technique is not productive because significance levels of the weaker lines become increasingly difficult to determine. There is the additional difficulty of confusion between various lines through their side-band components (Fig. 4d), which makes the cleaning process inefficient and results in uncertain amplitudes for weaker lines. In order to gain a clearer view of the frequency composition of the optical data, we have in the following analysis taken advantage of the nature of the discrete line structure apparent in the power spectrum, the fact that the important frequencies appear to be sums and differences of harmonics of  $\nu_{1.7}$  and  $\nu_{35}$ .

#### c) Harmonic Analysis

Figure 2 may be interpreted as a two-dimensional, toroidal representation of the optical flux data. A natural orthogonal set of functions which span this torus is just that composed of the products of the

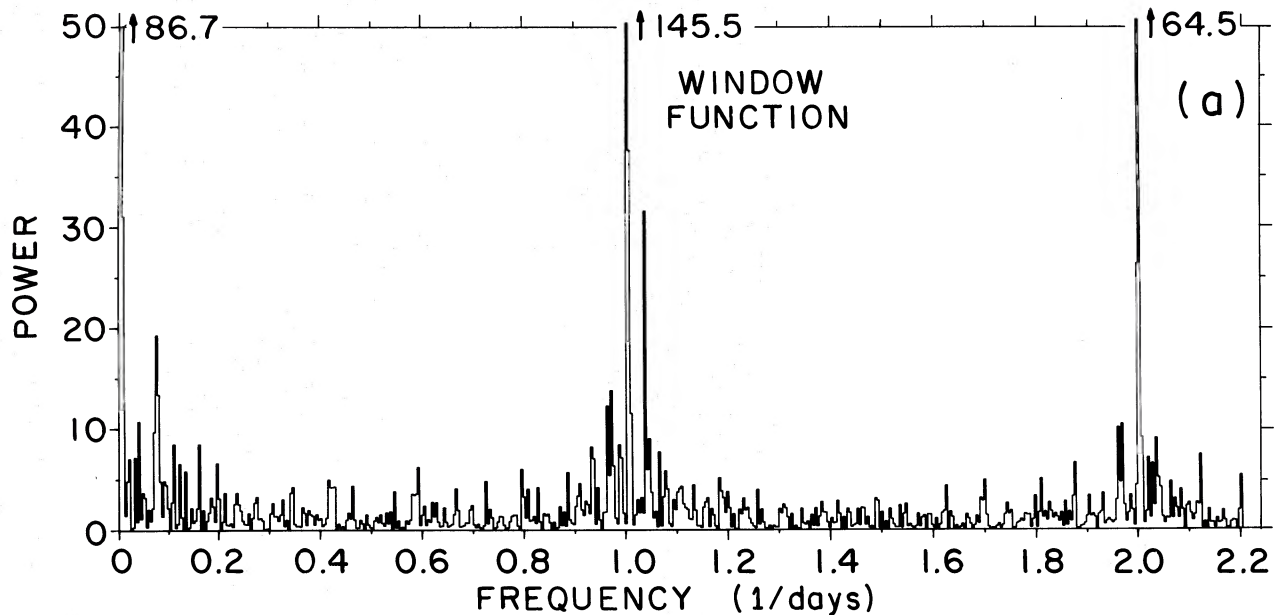


FIG. 4a.—Power spectrum of the window function for 1973 *B* data. Power density plotted in units of the average power density over the low-frequency half of the spectrum.

sines and/or cosines of the harmonics of  $\nu_{1.7}$  and  $\nu_{35}$  (or, equivalently, sines and cosines of sums and differences of harmonics of these frequencies). Of course, orthogonality holds only for uniformly distributed data; but with standard regression methods one can fit the data to the general sum of these mixed harmonic terms. The lack of orthogonality resulting from the irregular sampling is naturally reflected in the correlation matrix. This “harmonic fit” has two distinct advantages over standard spectral analysis for this

type of data: the confusion between lines resulting from correlations between line and side-band amplitudes is greatly reduced, and an error estimate (significance level) for each of the terms is readily determined. Table 1 summarizes the application of this procedure to *B* flux measured in the 1972–1974 observing seasons. The 946 points used in this analysis are those plotted in Figure 2. The epoch (point of zero phase) used in the harmonic analysis is arbitrary, so we may choose it to correspond to one of the four

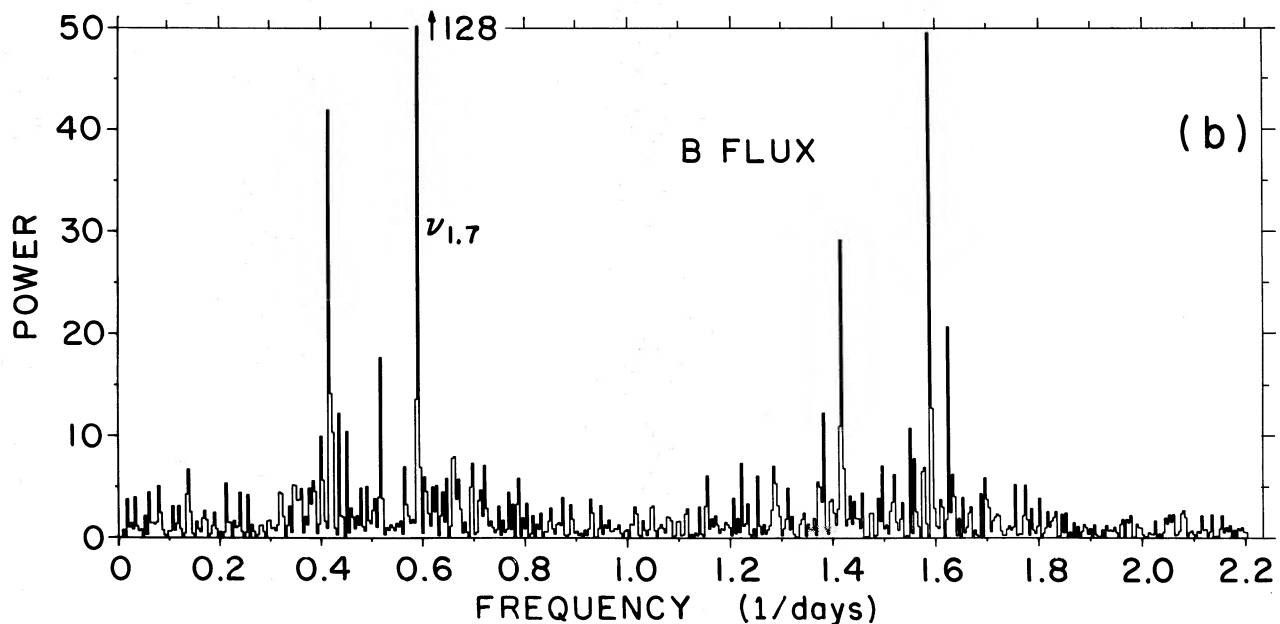


FIG. 4b.—Untouched power spectrum of 1973 *B* data. Power density defined as in Fig. 4a.

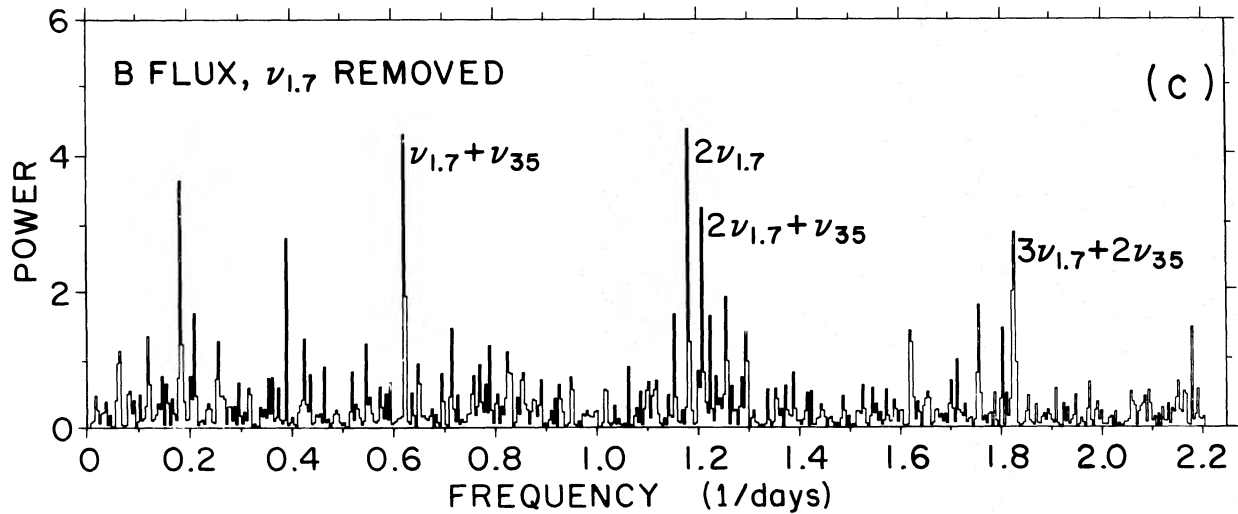


FIG. 4c.—Power spectrum with  $\nu_{1.7}$  term removed. Same power density scale as in Fig. 4b.

time-reversal symmetry points discussed in connection with Figure 2. These symmetry points are determined by varying the epoch to minimize the amplitude of the symmetry-violating sine terms. The actual epoch is associated with the same symmetry point as in the earlier discussion; it occurs in  $35^{\text{d}}$  phase,  $\Delta\psi = 0.150 \pm 0.005$  after X-ray turn-on, and in  $1^{\text{d}7}$  phase,  $\Delta\phi = 0.992 \pm 0.002$  after X-ray mideclipse. The coefficients in Table 1 result from applying the two-dimensional harmonic analysis with this epoch to all available  $B$  flux observations. Cosine terms clearly dominate. The only symmetry-violating term significant at the  $5\sigma$  level is  $\nu_{1.7} + 2\nu_{35}$ . Furthermore, only 2 percent of the total power is not contained in the harmonics listed. This residue is comparable to the expected measurement variance, demonstrating that the analysis using only harmonic terms in  $\phi$  and  $\psi$  is self-consistent.

The terms in Table 1 are summarized in Figure 5 as a flux contour diagram which reveals a strong diagonal ridge line that extends throughout the  $1^{\text{d}7}$  phase; because maximum flux occurs at midphase, this ridge is most visible as a central peak in the light curve during the X-ray OFF period. There is also a

second, weaker diagonal ridge line which is broken at midorbital phase by the secondary minimum. In addition, one finds a noticeable  $17^{\text{d}5}$  period in width of primary minimum resulting from the successive eclipsing of each ridge.

### III. COLOR ANALYSIS

If the harmonic analysis is applied to  $U$ ,  $B$ , and  $V$  fluxes separately, the colors of corresponding coefficients should contain information about the color variation throughout the light curve. In particular, if the  $35^{\text{d}}$  variation is related to a source with a characteristic color, that color should be readily identified in the terms involving  $35^{\text{d}}$  periodicity. Unfortunately, this color "signature" is not distinctive, since all the significant terms involving  $35^{\text{d}}$  periodicity have colors in the range  $-0.95 > U - B > -1.10$ , and are only marginally bluer than the color of the dominant  $1^{\text{d}7}$  variation ( $U - B = -0.96$ ).

There is one striking exception to the narrow range of colors given above. The second harmonic term,  $2\nu_{1.7}$ , has colors  $U - B = +0.7 \pm 0.4$ ,  $B - V = +0.2 \pm 0.1$ —reminiscent of the colors of the cool face

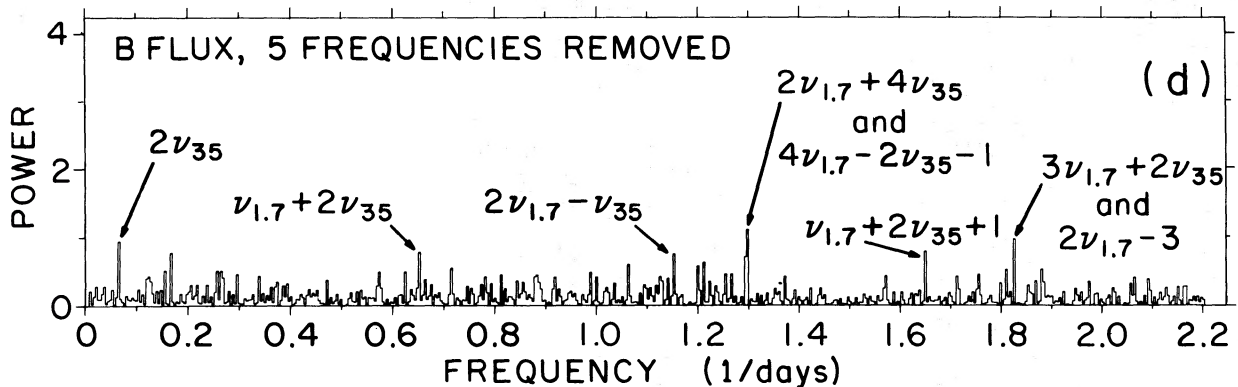


FIG. 4d.—Power spectrum further cleaned by the removal of five dominant terms. Same power density scale as in Fig. 4b.

TABLE 1  
AMPLITUDES OF HARMONIC COMPONENTS  
OF  $B$  FLUX

HARMONIC*		AMPLITUDE**	
$m$	$n$	Cos Term	Sin Term
0	0	+3.92	...
1	0	-2.16	0.00
2	0	-0.26	+0.02
3	0	+0.04	0.00
4	0	-0.15	0.00
0	+1	+0.02	0.00
1	+1	+0.31	+0.02
2	+1	-0.29	-0.02
3	+1	+0.03	+0.04
4	+1	-0.04	-0.01
1	-1	+0.03	+0.04
2	-1	-0.10	-0.02
3	-1	+0.05	+0.03
4	-1	-0.02	-0.02
0	+2	+0.14	+0.02
1	+2	+0.10	-0.11
2	+2	+0.16	+0.02
3	+2	-0.31	+0.04
4	+2	-0.02	-0.03
1	-2	+0.05	-0.03
2	-2	-0.09	+0.01
3	-2	+0.05	-0.02
4	-2	-0.12	-0.03

\* Frequency  $\nu_{mn} = m\nu_{1.7} + n\nu_{35}$ .

\*\* The  $5\sigma$  (rms) level is 0.07, except for the constant term, for which it is 0.05.

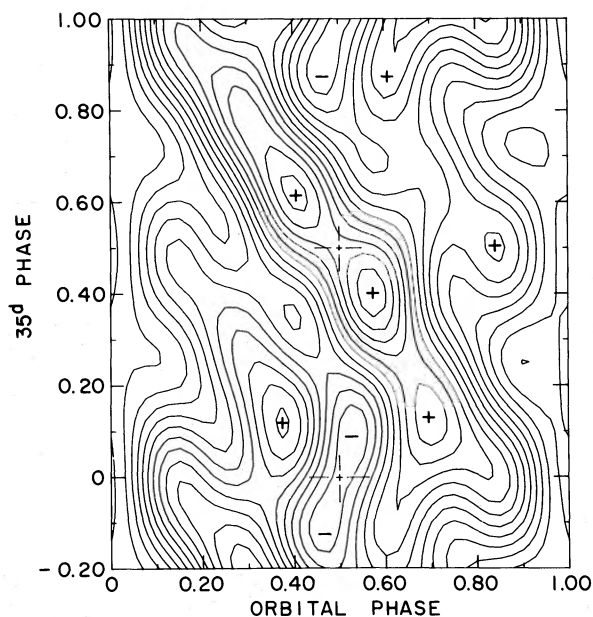


FIG. 5.—Contour plot of  $B$  flux over 197 phase by  $35^d$  phase. Contour levels are at intervals of 0.2 flux units; pluses denote local maxima; minuses denote minima. Horizontal cuts on this diagram represent a smoothed version of the data shown in Fig. 2. The two symmetry points at  $\phi \approx 0.5$  are shown as crosses.

of HZ Her at primary minimum. Furthermore, the inferred full amplitude (0.34 mag) of the  $2\nu_{1.7}$  term is only slightly larger than that observed during the extended OFF state (Forman, Jones, and Liller 1972). These similarities suggest that this term is due to gravity darkening, but this possibility is extremely difficult to reconcile with the physical conditions associated with X-ray heating. An alternative interpretation, which is more compatible with the “half-illuminated” model, is to regard the  $2\nu_{1.7}$  term as a continuous color correction to the basic  $\nu_{1.7}$  term in the light curve. Since the two terms are both negative and the second harmonic is “cooler” than the first harmonic (i.e., affects  $U$  less than  $B$  and  $V$ ), the sum of the two terms will result in a component which is hotter at midphase than at primary minimum.

More precise information about the range and location of color variations in the light curve may be obtained by applying the technique described in Boynton *et al.* (1973) to calculate differential colors for subsets of the data. This approach determines the colors for changes in the flux, rather than the raw colors based on total fluxes. The result of applying this analysis to 86 individual nights is shown in Figure 6. The scatter near midphase is partly due to the low stability of the differential method where the slope is small, but there is also a correlation with  $35^d$  phase: the bluest points occur near the brightest feature in the light curve (compare Fig. 5). Otherwise, Figure 6 indicates a smooth variation from coolest at primary minimum to hottest at midorbital phase. This is qualitatively what would be expected from a naïve model based solely on X-ray illumination.

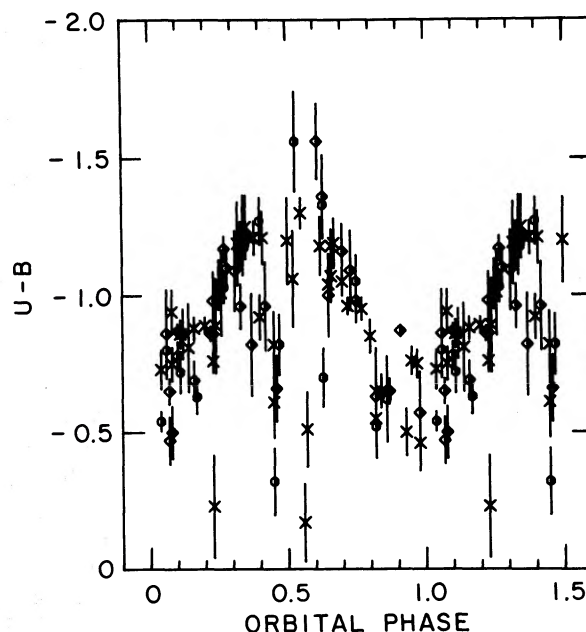


FIG. 6.— $U - B$  differential colors for individual nights, calculated by the method described in the text. Our data are indicated by  $\times$ ; data of Grandi *et al.* (1974) by  $\diamond$ ; and data of Chevalier and Ilovaisky (1974b) by  $\circ$ . Estimated  $1\sigma$  (rms) error limits are indicated by bars.

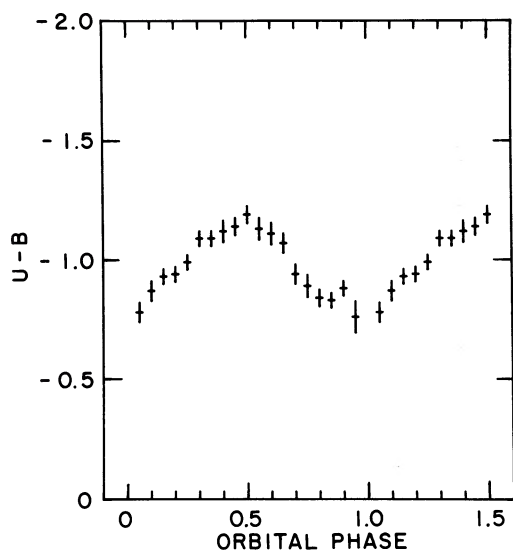


FIG. 7.— $U - B$  differential colors for intervals in  $1^{d7}$  phase. Each bar represents data from an interval of width 0.1 in  $1^{d7}$  phase; the length of the bar corresponds to  $1 \sigma$  rms.

A different approach is to eliminate the basic  $1^{d7}$  component in the light curve by applying the above analysis to data contained in narrow intervals in  $1^{d7}$  phase. The result of this calculation, which determines the colors of the  $35^d$  variation at fixed  $1^{d7}$  phase, is shown in Figure 7. The two approaches summarized in Figures 6 and 7 yield strikingly similar curves, indicating that the  $35^d$  variation probably involves the same process which gives rise to the basic  $1^{d7}$  light curve (e.g., the X-ray illuminated model). The absence of a distinct color for the  $35^d$  variations also explains the failure of the harmonic analysis on  $U, B, V$  fluxes to isolate a  $35^d$  color "signature."

#### IV. DISCUSSION

The following six points summarize the basic properties of light curve structure indicated by the analysis discussed in the previous sections:

- The pattern in variation of optical flux is remarkably repeatable from one  $35^d$  cycle to the next.
- The maximum amplitude of these systematic flux variations is roughly half the maximum amplitude of the  $1^{d7}$  Fourier components of the light curve.
- The time dependence of this structure is dominated by frequency components corresponding to the mixed harmonics of  $\nu_{1.7}$  and  $\nu_{35}$ , such as  $\nu_{1.7} + \nu_{35}$ ,  $2\nu_{1.7} + \nu_{35}$ , and  $3\nu_{1.7} + 2\nu_{35}$ .
- Independently of the frequency composition of the light curve structure, the phases of the various terms indicate a highly significant  $35^d$  symmetry in the evolution of the light curve. That symmetry is related to the X-ray cycle through the location of the optical symmetry points  $\psi = 0.0$  and  $0.50$ :  $\psi \approx -0.15$  corresponds to nominal X-ray turn-on.
- The secondary minimum, although not part of

the moving pattern, does participate in the  $35^d$  symmetry by being centered on  $\psi = 0.0$ .

f) A significant  $\nu_{35}$  component is conspicuously absent in the harmonic analysis of the optical flux. The  $5 \sigma$  upper limit on its amplitude is less than 4 percent of the amplitude of the  $1^{d7}$  variation.

There have been two fundamental problems in dealing with the light curve of HZ Her: explaining the sharp, narrow primary minima (Wilson 1973; Joss, Avni, and Bahcall 1973), and understanding the amplitude of the overall  $1^{d7}$  flux change in terms of a credible energy budget (Avni *et al.* 1973; Milgrom and Salpeter 1975; Perrenod and Shields 1975). In a phenomenological sense, the discovery of periodic, large-amplitude flux changes which drift in  $1^{d7}$  phase "explains" the sharp primary minima which are seen to occur every 17.5 days. These same features, which may be distinct in origin from the underlying  $1^{d7}$  variation (there is a mild color difference), also may mitigate the energy problem by allowing a significant fraction of the flux to be produced in a region other than the heated face of the primary. In any case, it seems a useful concept that the transient shoulders, bumps, or irregularities of earlier discussions can be understood (with the benefit of data from many observers as pooled in this paper) to arise from a single, systematic progression of features which persist throughout  $35^d$  and  $1^{d7}$  phase (except at primary minimum).

The strong indications of amplitude modulation and/or additive mixing of harmonics of  $\nu_{1.7}$  and  $\nu_{35}$ , along with the impressive  $35^d$  symmetry and high degree of repeatability in the evolution of the light curve, argue for a distinctly geometrical model consisting of several moving, luminous regions whose changing aspect results in the observed flux variations. In fact, the "time-reversal" symmetry of the optical curves argues against alternatives such as a  $35^d$  relaxation process which might involve changing mass-transfer or accretion rates, changing accretion-disk dimensions (and hot-spot position), and consequently a system luminosity which evolves but repeats every 35 days (Pines, Pethick, and Lamb 1973).

A geometrical interpretation leads to the possibility that the dominant  $\sim 1^{d6}$  mixed term ( $\nu_{1.7} + \nu_{35}$ ) and conceivably the  $2\nu_{1.7} + \nu_{35}$  and  $3\nu_{1.7} + 2\nu_{35}$  terms, result from the following simple coupling of the  $1^{d7}$  orbital period and the  $35^d$  component of the system: suppose the  $35^d$  variation stems from a simple rotation of the X-ray source radiation pattern about an axis normal to the orbital plane. This rotation might result from a precession of the source itself or the precession of a partially obscuring accretion disk. For  $35^d$  precession in the *opposite* sense to the orbital motion (consistent with forced precession), the same relative orientation of source pattern and companion star occurs every  $\sim 1.6$  days. This periodic occurrence could result in a corresponding modulation of optical flux. It is also possible to imagine how the mass transfer may depend on this relative orientation, thereby producing the nominal 1.6 day recurrence of the X-ray absorption dips. In a subsequent paper we

define a class of simple geometrical models which can quantitatively account for this optical behavior and may imply additional specific properties for the accretion disk.

This work was supported in part by NSF grant number AST75-07769.

## REFERENCES

- Avni, Y., Bahcall, J. N., Joss, P. C., Bahcall, N. A., Lamb, F. K., Pethick, C. J., and Pines, D. 1973, *Nature Phys. Sci.*, **246**, 36.
- Boynton, P. E., Canterna, R., Crosa, L., Deeter, J., and Gerend, D. 1973, *Ap. J.*, **186**, 617.
- Chevalier, C. and Ilovaisky, S. A. 1973, *Nature Phys. Sci.*, **245**, 87.
- . 1974a, *Astr. and Ap.*, **35**, 407.
- . 1974b, private communication.
- Davidsen, A., Henry, J. P., Middleditch, J., and Smith, H. E. 1972, *Ap. J. (Letters)*, **177**, L97.
- Forman, W., Jones, C. A., and Liller, W. 1972, *Ap. J. (Letters)*, **177**, L103.
- Grandi, S. A., Hintzen, P., Jensen, E., Rydgren, A., Scott, J., Stickney, P., Whelan, J., and Worden, S. 1974, *Ap. J.*, **190**, 365.
- Joss, P. C., Avni, Y., and Bahcall, J. N. 1973, *Ap. J.*, **186**, 767.
- Kurochkin, N. E. 1972, *Variable Stars*, Vol. 18, No. 5, p. 425.
- . 1973, *Inf. Bull. Var. Stars*, No. 753.
- Lyutiy, V. M., Sunyaev, R. A., and Cherepashchuk, A. M. 1973, *Astr. Zh.*, **50**, 3.
- . 1974, *ibid.*, **51**, 1150.
- Milgrom, M., and Salpeter, E. E. 1975, *Ap. J.*, **196**, 589.
- Perrenod, S. C., and Shields, G. A. 1975, *Ap. J.*, **198**, 153.
- Petro, L., and Hiltner, W. A. 1973, *Ap. J. (Letters)*, **181**, L39.
- Pines, D., Pethick, C., and Lamb, F. 1973, *Ann. New York Acad. Sci.*, **224**, 237.
- Wilson, E. R. 1973, *Ap. J. (Letters)*, **181**, L75.

P. E. BOYNTON, L. CROSA, J. DEETER, and D. GEREND: Department of Astronomy, FM-20, University of Washington, Seattle, WA 98195